Eur. Phys. J. C 24, 529–533 (2002)
Digital Object Identifier (DOI) 10.1007/s10052-002-0973-3

THE EUROPEAN PHYSICAL JOURNAL C

Self-similar properties of the proton structure at low x

T. Laštovička[1,2,a]

[1] DESY Zeuthen, Platanenallee 6, 15738 Zeuthen, Germany
[2] Charles University, Faculty of Mathematics and Physics, V Holešovičkách 2, 18000 Prague 8, Czech Republic

Received: 28 March 2002 /
Published online: 21 June 2002 –

Abstract. Self-similar properties of proton structure in the kinematic region of low values of the Bjorken variable x are introduced and studied numerically. A description of the proton structure function $F_2(x, Q^2)$ reflecting self-similarity is proposed with a few parameters which are fitted to recent HERA data. The specific parametrisation provides an excellent description of the data which cover the region of four momentum transfer squared $0.045 \leq Q^2 \leq 120\,\mathrm{GeV}^2$, and of the Bjorken variable x $6.2 \cdot 10^{-7} \leq x \leq 0.01$.

1 Introduction

Recent measurements of the H1 [1] and ZEUS [2] collaborations at HERA enable one to study the proton structure in the region of low $Q^2 \lesssim 1\,\mathrm{GeV}^2$, where perturbative QCD has to face computation difficulties arising from the increase of the strong coupling constant $\alpha_\mathrm{s}(Q^2)$. Nevertheless, there are a number of approaches to describe the transition to low Q^2 at small x together with the region $Q^2 > 1\,\mathrm{GeV}^2$, which is described by perturbative QCD very well. Such attempts involve reggeon exchange ideas [3], dipole interactions [4], vector meson dominance (VMD) [5], efficient parametrisations [6] and others.

This letter presents a different point of view, based on the idea that the proton structure at low x is of fractal nature[1]. Using the fractal dimension concept [8], a simple parametrisation of the proton structure function $F_2(x, Q^2)$ is obtained with a few well-defined parameters. A numeric study is made using recent small x HERA data for Q^2 between $0.045\,\mathrm{GeV}^2$ and $120\,\mathrm{GeV}^2$.

2 Fractal dimension

The concept of fractal dimension requires one to understand what is meant by *dimension*. In non-fractional dimensions the number of dimensions corresponds to the number of independent directions in a corresponding coordinate system. For example, a line has obviously one dimension, a square two and a cube has three dimensions. The dimension of the Sierpinski gasket [9], shown in Fig. 1, needs a more general definition.

The cube, square and line are *self-similar* objects: when a line is broken in the middle two lines are obtained, each of half length. By magnifying one of them by a factor of two the original line is rebuilt. The same may be done by dividing a square into four small squares or a cube into smaller cubes. For example, when the magnification factor for a square is 3 the number of smaller squares will be $3^2 = 9$; for a cube the same magnification gives $3^3 = 27$ cubes. In general, when M is the magnification factor, then the number of objects will be $M^\mathcal{D}$, where $\mathcal{D}$ is the dimension of the object. The dimension $\mathcal{D}$ can thus be defined by

$$\mathcal{D} = \frac{\log M^\mathcal{D}}{\log M} = \frac{\log(\text{number of self-similar objects})}{\log(\text{magnification factor})}. \quad (1)$$

According to this formula, the dimension of the Sierpinski gasket is fractional. When the magnification factor M is 2 there are three identical pieces of the gasket, for $M = 4$ the gasket consists of nine small copies of itself. Therefore its fractal dimension is defined by

$$\mathcal{D} = \frac{\log 3}{\log 2} = \frac{\log 9}{\log 4} = 1.58496\ldots \quad (2)$$

Roughly speaking, the fractal dimension describes how complicated or how large a self-similar object is. A plane is "larger" than a line. The Sierpinski gasket is not a line but

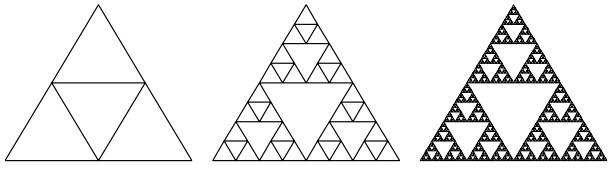

Fig. 1. Sierpinski gasket fractal in iterations No. 1, 3 and 6 (from left). Iteration No. 1 corresponds to the *seed image* which is arbitrary while the iteration always converges to the same object

[a] e-mail: lastovic@ifh.de

[1] A related approach employing self-organised criticality was proposed in [7].

also far from being a plane. Actually, there exist fractals which are constructed from lines but have dimensions 2 or 3, and therefore fill a plane or a space. An example of such a curve is the so-called Hilbert curve.

The definition of a dimension, given in (1), may be generalised for the case of non-discrete fractals. In this generalisation, the magnification (scaling) factor is a real number z and the number of self-similar objects is represented by a density function $f(z)$. Taking into account that the dimension may change with scaling, the *local dimension* is defined by

$$\mathcal{D}(z) = \frac{\partial \log f(z)}{\partial \log z}. \tag{3}$$

For ideal mathematical fractals, as discussed so far, $\mathcal{D}(z)$ is constant for the whole fractal. Introducing a scale dependent dimension is natural because many fractals in nature (e.g. plants or coastlines) are not mathematically ideal and usually have a fractal structure only for a certain region of magnification. In such a region, the dimension is approximately constant, $\mathcal{D}(z) = \mathcal{D}$, and, following (3), the density function $f(z)$ is given by

$$\log f(z) = \mathcal{D} \cdot \log z + \mathcal{D}_0, \tag{4}$$

where $\mathcal{D}_0$ defines the normalisation of $f(z)$, which thus has a *power law* behaviour, $f(z) \propto z^D$.

In general, fractals may have two *independent* magnification factors, z and y. In this case the density $f(z, y)$ is written in the following way:

$$\begin{aligned}\log f(z,y) = \mathcal{D}_{zy} \cdot \log z \cdot \log y + \mathcal{D}_z \cdot \log z \\ + \mathcal{D}_y \cdot \log y + \mathcal{D}_0.\end{aligned} \tag{5}$$

Here the dimension $\mathcal{D}_{zy}$ represents the dimensional correlation relating the z and y factors. The function $f(z, y)$ satisfies a power law behaviour in z for fixed y and in y for fixed z.

It is important to mention that there is a certain freedom in selecting magnification factors without changing the shape of the function $f(z, y)$. It is possible to use any non-zero power of a factor multiplied by a constant: $z \to az^\lambda$. The only effect of such a change is a redefinition of the dimensional parameters $\mathcal{D}_{\{z,y,zy\}}$ and of the normalisation $\mathcal{D}_0$, respectively.

3 Self-similar structure of the proton

Following the dimensional description of the fractal structures presented, it is interesting to study the properties of functions describing the proton structure. In quantum chromodynamics the behaviour of the sea quark densities is driven by gluon emissions and splittings. The deeper the proton structure is probed, the more gluon–gluon interactions can be observed. These, in analogy to fractals, may follow self-similarity, i.e. scaling described by a power law. Indeed, there are a number of hints for a self-similar structure. As an example, Fig. 2 shows the unintegrated

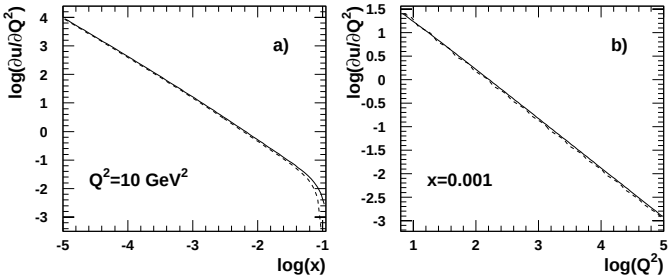

Fig. 2a,b. Logarithm of the unintegrated u-quark density $\partial u(x, Q^2)/\partial Q^2$ as a function of the Bjorken variable x **a** and Q^2 **b**. The full and dashed lines correspond to GRV parametrisations in LO and NLO [10], respectively

u-quark density for fixed momentum transfer Q^2 and fixed Bjorken variable x, respectively. For $x \lesssim 0.01$ (below the valence quark region) the unintegrated density function in log–log scale is linear. A linear behaviour is also exhibited by the unintegrated density as a function of Q^2 for fixed x. Referring to (4), this suggests that x and Q^2 could be treated as appropriate magnification (scaling) factors. This is support for the idea that the proton structure exhibits self-similar properties and may be described as a fractal object.

Magnification factors are supposed to fulfil some criteria. They should be positive, non-zero and have no physical dimension. The two latter requirements concern the selection of Q^2 as a magnification factor. The physical dimensionality may be removed by dividing Q^2 by a constant Q_0^2. For the case of $Q^2 = 0$, the non-zero requirement is not fulfilled; however, the access to this region is needed for the integration of unintegrated densities. Thus instead of Q^2 the choice of $1 + Q^2/Q_0^2$ as a magnification factor is appropriate. According to the freedom in the magnification factor selection, mentioned above, other equivalent choices are also possible, e.g. $Q_0^2/(Q_0^2 + Q^2)$, $(Q_1^2 + Q^2)/1\,\mathrm{GeV}^2$ or similar combinations. It is also more appropriate to use $1/x$ as a magnification factor rather than x itself: when the structure is probed deeper, x goes to zero while the magnification factor should increase.

4 Structure function parametrisation

The concept of self-similarity, when applied to the proton confinement structure, leads to a simple parametrisation of the quark densities within the proton in a straightforward way based on (5). Using magnification factors $1/x$ and $1 + Q^2/Q_0^2$, the unintegrated quark density may be written in the following general form:

$$\begin{aligned}\log f_i(x, Q^2) = \mathcal{D}_1 \cdot \log \frac{1}{x} \cdot \log\left(1 + \frac{Q^2}{Q_0^2}\right) + \mathcal{D}_2 \cdot \log \frac{1}{x} \\ + \mathcal{D}_3 \cdot \log\left(1 + \frac{Q^2}{Q_0^2}\right) + \mathcal{D}_0^i,\end{aligned} \tag{6}$$

where i denotes the quark flavour. Conventional, integrated quark densities $q_i(x, Q^2)$ are defined as a sum over

Table 1. Results of the fit. The first row corresponds to a fit to all parameters; in the second row the parameter $\mathcal{D}_2$ was fixed to 1

	$\mathcal{D}_0$	$\mathcal{D}_1$	$\mathcal{D}_2$	$\mathcal{D}_3$	Q_0^2 [GeV^2]
all fit	0.339	0.073	1.013	−1.287	0.062
	±0.145	±0.001	±0.01	±0.01	±0.01
$\mathcal{D}_2$ fixed	0.523	0.074	*1*	−1.282	0.051
	±0.014	±0.001	const.	±0.01	±0.002

Table 2. Results of the fit, summarised in terms of χ^2. The number of F_2 data points is 172; total errors were used for the χ^2 calculation

	χ^2	χ^2/ndf
all fit	136.6	0.82
$\mathcal{D}_2$ fixed	138.4	0.82

all contributions with quark virtualities smaller than that of the photon probe, Q^2. Thus $f_i(x, Q^2)$ has to be integrated over Q^2,

$$q_i(x, Q^2) = \int_0^{Q^2} f_i(x, q^2) \mathrm{d}q^2. \tag{7}$$

Solving equation (7), the following analytical parametrisation of a quark density is obtained:

$$q_i(x, Q^2) = \frac{\mathrm{e}^{\mathcal{D}_0^i} Q_0^2 x^{-\mathcal{D}_2}}{1 + \mathcal{D}_3 - \mathcal{D}_1 \log x} \times \left(x^{-\mathcal{D}_1 \log(1+(Q^2/Q_0^2))} \left(1 + \frac{Q^2}{Q_0^2}\right)^{\mathcal{D}_3+1} - 1 \right). \tag{8}$$

Notice that in this parametrisation only the normalisation parameter $\mathcal{D}_0^i$ depends on the quark flavour while the other parameters are flavour independent. This assumption means that all quarks are following the fractal structure, i.e. the dimensions D_i and the magnification factors are common for all of them and they differ in normalisation only.

The proton structure function $F_2(x, Q^2)$ is related directly to the quark densities $F_2 = x \sum_i e_i^2 (q_i + \bar{q}_i)$. Thus the assumption about the flavour symmetry of (8) allows one to express $F_2(x, Q^2)$ directly in the form given on the r.h.s. of (8) with $x^{-\mathcal{D}_2}$ replaced by $x^{-\mathcal{D}_2+1}$ and with a common normalisation factor $\mathrm{e}^{\mathcal{D}_0}$:

$$F_2(x, Q^2) = \frac{\mathrm{e}^{\mathcal{D}_0}\ Q_0^2\ x^{-\mathcal{D}_2+1}}{1 + \mathcal{D}_3 - \mathcal{D}_1 \log x} \times \left(x^{-\mathcal{D}_1 \log(1+(Q^2/Q_0^2))} \left(1 + \frac{Q^2}{Q_0^2}\right)^{\mathcal{D}_3+1} - 1 \right). \tag{9}$$

5 Fit to the data

The five parameters $\mathcal{D}_i$ and Q_0^2 are determined using recent data from the HERA experiments H1 [1] and ZEUS [2] in the range $1.5 \le Q^2 \le 120\,\mathrm{GeV}^2$ (H1) and $0.045 \le Q^2 \le 0.65\,\mathrm{GeV}^2$ (ZEUS). Additionally a cut $x < 0.01$ has been applied to exclude the valence quark region. The fit parameters are given in Tables 1 and 2, and the corresponding description of the $F_2(x, Q^2)$ data is shown in Figs. 3, 4 and 5. The χ^2 was calculated with total errors, adding the statistical and systematical errors in quadrature. When the relative normalisation of the H1 and ZEUS data, which cover different Q^2 regions, was fitted, no change beyond 1% was imposed by the fits. Thus the normalisations of the data sets were left untouched.

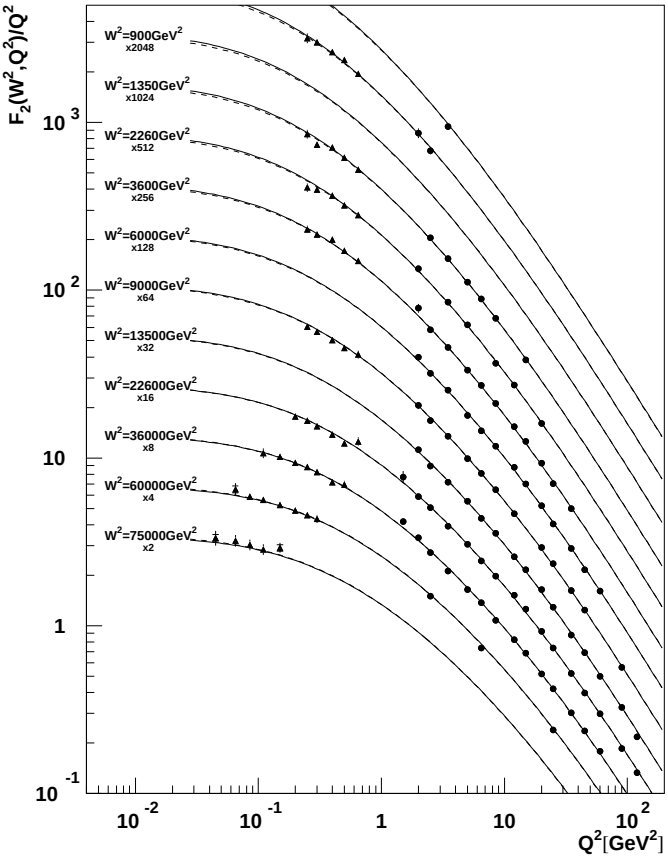

Fig. 3. Virtual photon–proton cross-section $\sigma_{\gamma^\star p} \propto F_2(W^2, Q^2)/Q^2$ as a function of Q^2 in W^2 bins. H1 (points) and ZEUS (triangles) measurements are shown along with the fit to four parameters (full line) and to all five parameters (dashed line)

Referring to Fig. 3 the ratio $F_2(W^2, Q^2)/Q^2$ is proportional to the virtual photon–proton cross-section $\sigma_{\gamma^\star p}(W^2, Q^2)$. In the limit $Q^2 \to 0$ and fixed W^2 the parametrisation (9) behaves like Q^2 only for $\mathcal{D}_2 = 1$. This may easily be shown e.g. when the unintegrated structure function $f(x, q^2)$ is introduced:

$$F_2(x, Q^2) = \int_0^{Q^2} f(x, q^2) \mathrm{d}q^2, \tag{10}$$

the parametrisation of which is identical to (6), with $\mathcal{D}_2$ replaced by $\mathcal{D}_2 - 1$ and $\mathcal{D}_0^i$ replaced by $\mathcal{D}_0$. If $F_2(x, Q^2)$ behaves like Q^2 for $Q^2 \to 0$ then $f(x, q^2)$ has to behave like

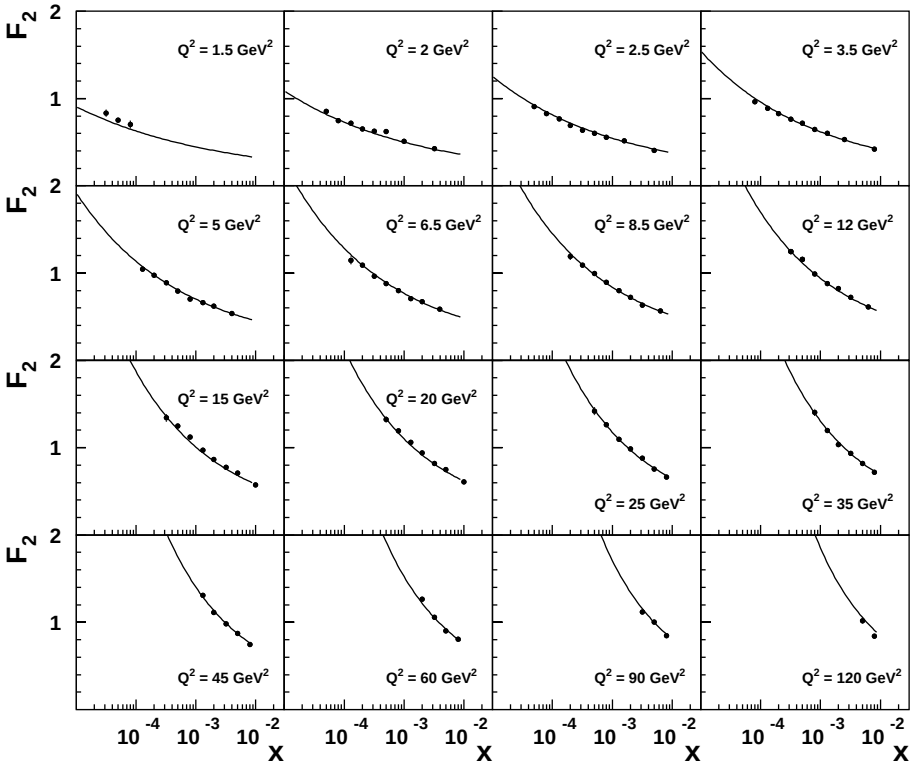

Fig. 4. Measurement of the structure function $F_2(x, Q^2)$ as a function of x in bins of Q^2 by the H1 experiment. The curve represents the fit to four parameters, which is indistinguishable from the five parameter fit in this kinematic region

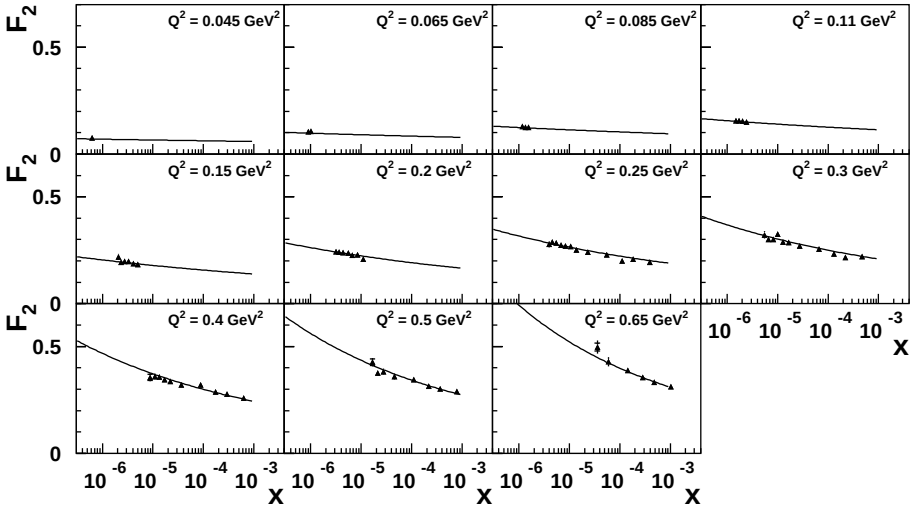

Fig. 5. Measurement of the structure function $F_2(x, Q^2)$ as a function of x in bins of Q^2 by the ZEUS experiment. The curve represents the fit to four parameters, which is indistinguishable from the five parameter fit in this kinematic region

a constant for any $x = Q^2/(W^2 - M_p^2) \to 0$. That is possible only if the divergent term, involving $\mathcal{D}_2$, is zero, i.e. for $\mathcal{D}_2 = 1$. In this case, since other logarithmic terms go to zero, the ratio $F_2(W^2, Q^2)/Q^2$ for $Q^2 \to 0$ approaches the value $\mathrm{e}^{\mathcal{D}_0}$.

In the fit with $\mathcal{D}_2$ as a free parameter a value very close to 1 is obtained. Thus a second fit was made, where $\mathcal{D}_2$ is fixed to 1 (see Tables 1 and 2, second row). This fit has four parameters and gives nearly the same χ^2/ndf as the first fit to all five parameters. Within the kinematic range of the F_2 data, both fits are nearly indistinguishable. As was stated above, the parameter $\mathcal{D}_0$ determines the virtual photon–proton cross-section in the photoproduction limit. Its value, obtained from the fit, gives

$$\sigma_{\gamma p} = \left[\frac{4\pi^2\alpha}{Q^2} F_2(W^2, Q^2)\right]_{Q^2 \to 0} \doteq 189 \pm 3\,\mu\mathrm{b}. \qquad (11)$$

This is in approximate agreement with the total photoproduction cross-sections measured by the H1 [11] and ZEUS [12] collaborations which were not used in the fit.

6 Summary

The concept of the self-similar structure of the proton was introduced. This leads to a parametrisation of the proton

structure function $F_2(x, Q^2)$ which describes very well the low x HERA data, both in the non-perturbative and the deep-inelastic domain. The introduced formalism uniquely defines the x and Q^2 dependence of parton densities; thus this approach is applicable also to other measures of proton structure, like the longitudinal structure function F_{L}, the diffractive structure function F_2^{D} or the spin structure function g_1.

Acknowledgements. I would like to express my gratitude to Max Klein and Krzysztof Golec-Biernat for fruitful discussions and careful reading of the manuscript. I am also very grateful to my family for the support.

References

1. H1: C. Adloff et al., Eur. Phys. J. C **21**, 33 (2001)
2. ZEUS: J. Breitweg et al., Phys. Lett. B **487**, 53 (2000)
3. A. Donnachie, P.V. Landshoff, Phys. Lett. B **518**, 63 (2001); A. Capella, E.G. Ferreiro, A.B. Kaidalov, C.A. Salgado, hep-ph/0106118; A. Capella, A. Kaidalov, C. Merino, J. Tran Thanh Van, In Meribel les Allues 1994, QCD and high energy hadronic interactions, pp. 271–282
4. K. Golec-Biernat, M. Wusthoff, Phys. Rev. D **59**, 014017 (1999)
5. G. Cvetic, D. Schildknecht, B. Surrow, M. Tentyukov, Eur. Phys. J. C **20**, 77 (2001)
6. D. Haidt, Nucl. Phys. Proc. Suppl. **96**, 166 (2001)
7. M. Ta-chung, R. Rittel, K. Tabelow, Gluons in small-x_{B} deep-inelastic scattering, hep-ph/9905538
8. Benoit B. Mandelbrot, The fractal geometry of nature (Freeman, New York 1977)
9. Waclaw Sierpinski, Sur une courbe dont tout point est un point de ramification, Compt. Rendus Acad. Sci. Paris **160**, 302 (1915) Michael F. Barnsley, Fractals everywhere, 2nd ed. (Academic Press Professional, 1993)
10. PDFLIB: The Parton Density Functions Library, Version 8.04, GRV sets 4 and 14(98), CERN
11. H1: S. Aid et al., Z. Phys. C **69**, 27 (1995)
12. ZEUS: J. Breitweg et al., Eur. Phys. J. C **7**, 609 (1999)